IOP PUBLISHING PHYSICS IN MEDICINE AND BIOLOGY

Phys. Med. Biol. **54** (2009) 1661–1672 doi:10.1088/0031-9155/54/6/017

The use of gel dosimetry to measure the 3D dose distribution of a $^{90}Sr/^{90}Y$ intravascular brachytherapy seed

G Massillon-JL[1,2], R Minniti[1], M G Mitch[1], M J Maryanski[3] and C G Soares[1]

[1] Ionizing Radiation Division, National Institute of Standards and Technology, Gaithersburg, MD 20899, USA
[2] Instituto de Física, Universidad Nacional Autónoma de México, AP 20-364, 01000 Distrito Federal, México
[3] MGS Research, Inc., Madison, CT 06443, USA

E-mail: massillon@fisica.unam.mx

Received 10 October 2008, in final form 16 January 2009
Published 25 February 2009
Online at stacks.iop.org/PMB/54/1661

Abstract

Absorbed dose distributions in 3D imparted by a single $^{90}Sr/^{90}Y$ beta particle seed source of the type used for intravascular brachytherapy were investigated. A polymer gel dosimetry medium was used as a dosemeter and phantom, while a special high-resolution laser CT scanner with a spatial resolution of 100 μm in all dimensions was used to quantify the data. We have measured the radial dose function, $g_L(r)$, observing that $g_L(r)$ increases to a maximum value and then decreases as the distance from the seed increases. This is in good agreement with previous data obtained with radiochromic film and thermoluminescent dosemeters (TLDs), even if the TLDs underestimate the dose at distances very close to the seed. Contrary to the measurements, $g_L(r)$ calculated through Monte Carlo simulations and reported previously steadily decreases without a local maximum as a function of the distance from the seed. At distances less than 1.5 mm, differences of more than 20% are observed between the measurements and the Monte Carlo calculations. This difference could be due to a possible underestimation of the energy absorbed into the seed core and encapsulation in the Monte Carlo simulation, as a consequence of the unknown precise chemical composition of the core and its respective density for this seed. The results suggest that $g_L(r)$ can be measured very close to the seed with a relative uncertainty of about 1% to 2%. The dose distribution is isotropic only at distances greater than or equal to 2 mm from the seed and is almost symmetric, independent of the depth. This study indicates that polymer gel coupled with the special small format laser CT scanner are valid

and accurate methods for measuring the dose distribution at distances close to an intravascular brachytherapy seed.

(Some figures in this article are in colour only in the electronic version)

1. Introduction

It is known that coronary artery disease is the main cause of death in the world (World Health Organization 2005). One of the possible techniques to treat this disease is angioplasty, during which a small balloon is used to open the narrowed artery. However, 30%–50% of patients undergo restenosis (renarrowing of the treated vessel) after angioplasty (King 1998, 1999). It is believed that, as in the treatment of pterygium or keloids, ionizing radiation can reduce the risk of narrowing caused by scar formation since it generally inhibits cell (smooth muscle cell) growth. Intravascular brachytherapy (IVBT) using beta or gamma emitters has been evaluated by randomized, controlled clinical trials and found to be a promising modality and a potential solution for prevention and treatment of restenosis (Brenner and Miller 2001, King 1998, Meerkin *et al* 1999). Based on these facts, different IVBT systems, which are considered as the most utilized in clinical trials in the United States, were approved by the Food and Drug Administration (FDA) (Chiu-Tsao *et al* 2007). One of these systems is the ^{90}Sr/^{90}Y beta source used in this work and developed by the Novoste Corporation[4]. In IVBT, the dose is prescribed at a fixed distance from the centre of the source depending on the radionuclide used and, for a given radionuclide, it varies with the vessel diameter (Meerkin *et al* 1999, Chiu-Tsao *et al* 2007).

As with gamma-emitting sources, beta-emitters exhibit very high dose rate gradients at close distances to the source, but unlike gamma emitters, insignificant doses at distances larger than 5 mm. These characteristics result in a great challenge to make accurate dose measurements. Thus, the continued use of beta-emitting sources in clinical applications (Ortolani *et al* 2005, Price *et al* 2007) and the concerns of guaranteeing a precise treatment of the patient have attracted the attention of more than one investigator. Various research groups have evaluated the dose distributions around these sources theoretically by Monte Carlo simulation (Asenjo *et al* 2002, Holmes *et al* 2006, Li *et al* 2000, Wang and Li 2000, 2002) or experimentally using thermoluminescent dosemeters and/or radiochromic film (Demir *et al* 2008, Duggan *et al* 1999, Holmes *et al* 2006, Roa *et al* 2004, Soares *et al* 1998). Until now, radiochromic film has been one of the most convenient techniques, which offers spatial resolution better than 0.1 mm in 2D (Chiu-Tsao *et al* 2007, ICRU 2004).

In the last decade, an alternative dosimetric system based on polymer gels has become available. These gels, called BANG (bis, acrylamide, nitrogen and gelatin) gels, are based on the radiation-induced polymerization of acrylic monomers dispersed in an aqueous gel, and were proposed by Maryanski and collaborators (Maryanski *et al* 1993) and used to measure the three-dimensional (3D) absorbed dose distribution imparted during radiotherapy treatment with high spatial resolution (Maryanski *et al* 1994, 1996). In this study, a new formulation of BANG gel named BANG3-Pro-1, based on the radiation-induced polymerization of methacrylic acid and specially made for high-ionization dosimetry (Massillon-JL *et al* 2008,

[4] Certain commercial equipment, manufacturers, instruments, or materials are identified this paper in order to specify the experimental procedure adequately. Such identification is for informational purposes only and is not intended to imply recommendation or endorsement by the National Institute of Standards and Technology, nor is it intended to imply that the manufacturer, materials or equipment are necessarily the best available for the purpose.

2009), was used to measure the 3D dose distributions around a 5F Novoste Beta-Cath $^{90}Sr/^{90}Y$ single seed source. In particular, we evaluated the radial dose function, $g_L(r)$, according to the recommendations given in the TG-149 protocol (Chiu-Tsao *et al* 2007). To quantify the data, a high-resolution laser computer tomography (CT) scanner was used.

2. Materials and methods

2.1. The $^{90}Sr/^{90}Y$ beta source

The beta emitting parent/daughter pair $^{90}Sr/^{90}Y$ is one of the most used beta sources in medicine due to its long half-life and its high energy, which make it more penetrating. ^{90}Sr has a half-life of 28.8 y and is a pure beta emitter with a maximum energy of 546 keV. The daughter isotope, ^{90}Y is also a pure beta emitter whose maximum energy is 2.28 MeV and has a very short half-life of 64 h (Browne 1997). Due to their low-energy, the ^{90}Sr betas are mostly absorbed by the stainless steel encapsulation and the surrounding catheter. Thus, the therapeutic dose is delivered mainly by the ^{90}Y beta particles (Chiu-Tsao *et al* 2007). The 5 F Novoste Beta-Cath $^{90}Sr/^{90}Y$ single source has a 2.5 mm length, 0.56 mm diameter ceramic core encapsulated in a cylindrical stainless steel capsule with 0.04 mm walls and 0.05 mm ends (Chiu-Tsao *et al* 2007).

2.2. Gel phantom for irradiation with the seed

The polymer gel (BANG3-Pro-1, MGS Research Inc., Madison, CT) phantoms used in this work were prepared by the manufacturer. The main characteristics of this polymer gel have been studied previously and reported elsewhere (Massillon-JL *et al* 2009). In particular the gel response was found to be a dose rate independent up to 1 Gy min^{-1}, consistent with previous measurements performed by one of the co-authors (MJM) who found same results up to 7 Gy min^{-1}. Similar results have been observed with this same gel elsewhere (Zeidan 2009) for dose rates up to 10 Gy min^{-1}. Due to the relatively high dose rate that is characteristic of the $^{90}Sr/^{90}Y$ seed, the low-sensitivity gel, whose response is well known up to 275 Gy, was utilized. For the insertion of the seed, a thin barex (acrylonitrile/methylacrylate copolymer) tube with a wall thickness of 200 μm was embedded inside the gel and sealed on a polymethyl methracrylate (PMMA) cylinder of 76.2 mm outside diameter, 3 mm wall thickness and 150 mm height. The embedding of the tube is done to avoid any scattering of the light not due to the micro particles formed in the gel during the irradiation process. This allows measurement of the dose at closer distances to the centre of the seed. To prevent the dose saturation effect in a given region of interest within a high dose rate gradient radiation field, the gel was irradiated with accumulated doses. To ensure that the seed was positioned reproducibly between irradiations, a catheter was inserted and fixed into the barex tube as a stop (blocker). Figure 1 displays the irradiated gel sealed inside of the PMMA cylinder with the catheter. The bright region observed in the centre of the gel container is a direct visualization of the effect of the irradiation in the gel in the vicinity of the source. In this way, the gel not only allows one to obtain the value of the dose at the reference point of 2 mm (dosemeter), but also provides a direct 3D image of the dose distribution (3D imaging device).

2.3. Irradiation and readout process

A given gel phantom was irradiated twice using the same seed. In order to be able to add the doses from the two irradiations, it was critical to reproduce both the irradiation conditions and the position of the gel inside the scanner. For this purpose, both reference

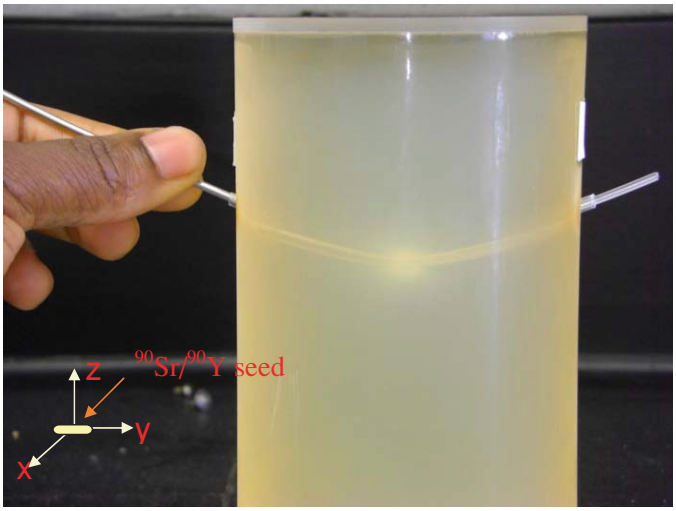

Figure 1. The gel after exposure to a ^{90}Sr/^{90}Y intravascular brachytherapy seed. The z-axis, the vertical axis of symmetry of the gel cylinder, corresponds to the radial distance from the seed.

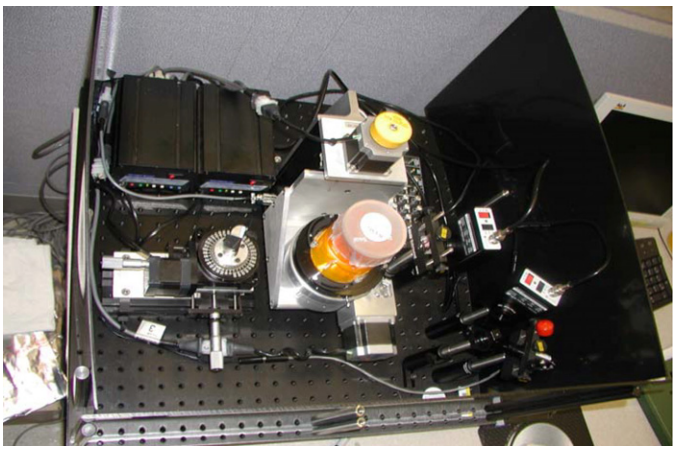

Figure 2. The laser CT scanner with an acrylic cylinder filled with polymer gel.

irradiation and readout geometries were defined. First, the gel was scanned using the laser CT scanner (DRYOCTOPUS, MGS Research Inc., Madison, CT) (Maryanski and Ranade 2001, Massillon-JL *et al* 2009) which is displayed in figure 2. To determine the un-irradiated gel response and any scattering of the laser by the embedded tube in the PMMA cylinder in the first slices close to the seed, a reference scan of 25 slices was taken with a resolution of 100 μm in all dimensions in this reference readout geometry. Meanwhile, the seed was marked with a permanent marker in order to identify its orientation with respect to the blocker position. Thereafter, two data sets were collected. First, the gel phantom was exposed for 135 min and afterward inserted into the scanner reference readout geometry. A total of 250 slices were obtained, over approximately 16 h, with the same resolution as the reference scan. The second irradiation was performed 3 d later for 127 min. Although we understood

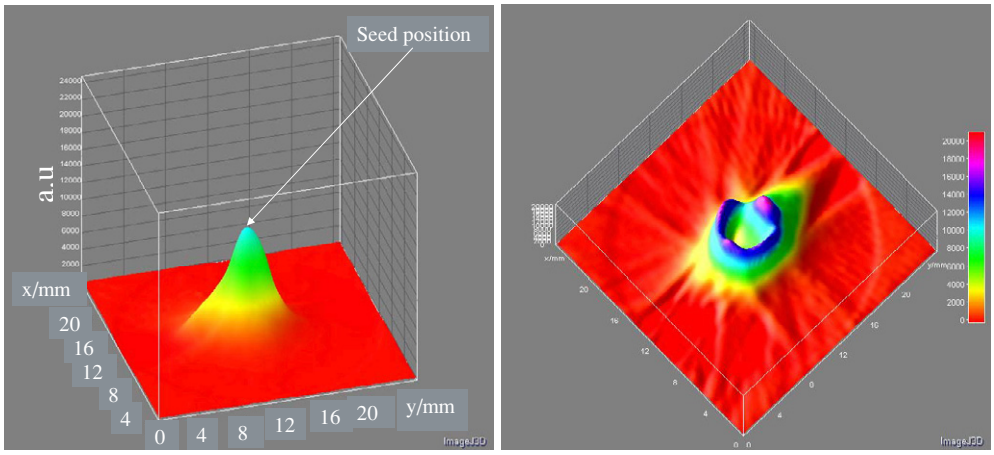

(a) (b)

Figure 3. (a) 3D surface scan reconstructed data of the dose distribution around a $^{90}Sr/^{90}Y$ beta seed obtained at 0.57 mm from the centre after exposure for 135 min. The z-axis corresponds to the intensity in the radial direction. (b) 3D surface scan reconstructed data of the dose distribution around the $^{90}Sr/^{90}Y$ beta seed after exposure for (135 + 127) min, viewed from the top. The z-axis corresponds to the intensity in the radial direction. The xy axis is the same as in figure 3(a) and the seed is positioned in the centre as is displayed in figure 3(a).

that the response of the gel at close distances to the seed might be affected by the saturation effect at very high dose, the second irradiation was made in order to obtain more accurate measurements at distances greater than 5 mm from the source. In addition, it is known that the gel response is reproducible and stable over the post-irradiation time as long as the response is linear (Massillon-JL *et al* 2009). Thus, in this case, the scan was performed immediately, and one week after the irradiation to better identify the time limits over which the gel response remains linear.

To reconstruct the map of optical attenuation coefficients, an image reconstruction program 'recon' written in MATLAB (The MathWorks, Natick, MA) was used and the analysis of the data was performed through the public-domain ImageJ software (ImageJ 2008).

3. Results

The relative 3D dose distribution for the $^{90}Sr/^{90}Y$ single seed measured at 0.57 mm from the seed centre is displayed in figures 3(a) and (b) for the 135 min and (135 + 127) min irradiation times, respectively. In both figures, the xy plane represents a cross section of the surface perpendicular to the vertical axis of symmetry of the gel cylinder shown in figure 1. The vertical axis represents the response of the gel expressed in arbitrary units and is directly proportional to the total dose. The value of the absorbed dose to water rate delivered at a radial distance of 2 mm is 1.8 Gy min^{-1}. The maximum dose at each point in the xy plane for the first irradiation of 135 min shown in figure 3(a) is well within the known response of the gel. A smooth transition from the maximum intensity value of 4000 arbitrary units near the seed down to zero for far distances can be observed. Figure 3(b) shows the effect of irradiating the same gel using the same seed a second time for an additional 127 min. This image was obtained 8 d post-irradiation. The first thing that can be noticed in figure 3(b) is that there is a depleted region around the centre with a radius of approximately 2 mm. A ring or circular

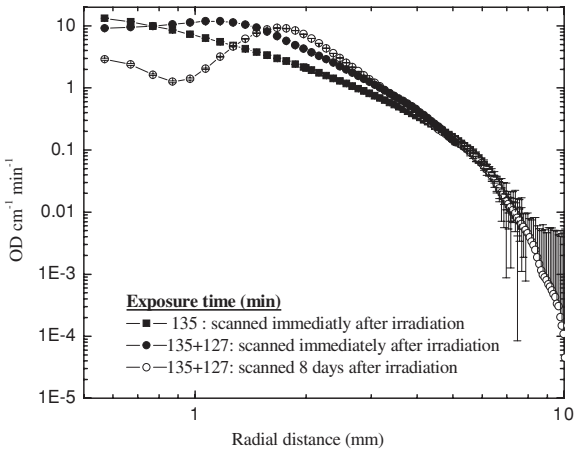

Figure 4. Normalized response of the polymer gel studied in this work (expressed in OD cm^{-1} min^{-1}) as a function of the radial distance from the $^{90}Sr/^{90}Y$ beta single source for both irradiation times. The combined standard uncertainties (for a coverage factor of $k = 1$) correspond to one standard deviation.

ridge is observed around the depleted region with much higher intensity. From that point on, the intensity decreases smoothly for increasing radial distance values. The depleted region observed in figure 3(b) is a combination of the saturation and the time post-irradiation effect. In the case of the saturation, the total dose delivered in this region of the gel from the first and second irradiation combined exceeds the maximum measurable dose of the dose–gel response curve. The post-irradiation time effect is probably due to a diffusion process of monomers from the low into high-dose region that are depleted by the polymerization reaction, given the dimension of the beta source and the very high dose gradient produced in a small region in the volume of the gel. However, for radial distances larger than 2 mm, the total dose delivered is still within the linear response range of the gel, and therefore a smooth decrease of the intensity is observed from the radial distance corresponding to the location of the ridge all the way out to the furthest distance from the seed.

Note that the axis transverse to the source corresponds to the vertical axis of symmetry of the cylindrical container containing the gel as shown in figure 1. The response of the gel along the transverse axis of the source was obtained by integrating each slice over an average area of 4 pixels $\times$ 4 pixels in the *xy* plane, which corresponds to 0.4 mm $\times$ 0.4 mm. The data matching was performed by normalizing the net gel (i.e., after background subtraction, using the reference scan) dose responses to their corresponding irradiation times. Figure 4 displays the normalized dose response of the gel expressed in units of OD cm^{-1} min^{-1} (optical density per cm per minute) as a function of the radial distance for both irradiation times: 135 min and (135 + 127) min. For the first irradiation, the response of the gel is well known (mostly linear) for all data points shown in the figure. Figure 4 also presents the effect of scanning the gel immediately, as well as 8 d after the gel was irradiated for the second irradiation. In both curves, a saturation effect can be observed for distances less than 4 mm by noticing the deviation from the curve corresponding to the first irradiation. This is expected since the dose delivered at the smaller distances is much higher than the value of the dose for which the gel-dose response is known (275 Gy). Furthermore, the saturated response changes with the time post-irradiation. As seen in the figure, this effect is larger when the gel is scanned

at a much later time (8 d) after the irradiation was completed. This was expected as reported in our previous work (Massillon-JL *et al* 2009). Based on this observation, the data in this region (distances smaller than 4 mm) are not included in the analysis described below. On the other hand for distances larger than 4 mm, there is a clear overlap between all three curves. This implies that the response of the gel in this region is not saturated and is linear. Using all the data in the linear range shown in figure 4, a radial depth dose curve was constructed. That is, for distances smaller than 5 mm only the data points of figure 4 from the first irradiation of 135 min was used. For larger distances, the data from the second irradiation were used instead, since they have a smaller standard deviation and therefore resulting in a lower uncertainty.

The radial dose function, $g_L(r)$, which quantifies the dose rate on the transverse axis at a distance r from the seed relative to the dose rate at a reference distance r_0, is defined as follows (Rivard *et al* 2004):

$$g_L(r) = \frac{\dot{D}\left(r, \frac{\pi}{2}\right)}{\dot{D}\left(r_0, \frac{\pi}{2}\right)} \frac{G_L\left(r_0, \frac{\pi}{2}\right)}{G_L\left(r, \frac{\pi}{2}\right)}, \tag{1}$$

where $G_L\left(r, \frac{\pi}{2}\right)$ is the geometry function, which describes the dose distribution in the absence of attenuation and scattering and is defined by the equation:

$$G_L\left(r, \frac{\pi}{2}\right) = \frac{\cos^{-1}\left(\frac{-L/2}{\sqrt{r^2+(L/2)^2}}\right) - \tan^{-1}\left(\frac{r}{L/2}\right)}{Lr}, \tag{2}$$

where L is the active length of the seed and equal to 2.5 mm (Chiu-Tsao *et al* 2007).

In this work, $\dot{D}\left(r, \frac{\pi}{2}\right)$ is the dose rate measured with the gel at a distance r, and is obtained from the radial depth dose curve built (not shown) as described above. According to the TG-60 protocol (Chiu-Tsao *et al* 2007), the reference distance r_0 is equal to 2 mm for beta-particle emitting seed sources. Following the TG-60 protocol, the first product ratio of equation (1) was obtained by normalizing the radial depth dose curve to unity at 2 mm. Figure 5 presents this result as a function of the radial distance from the centre of the seed. The radial dose function as well as its relative combined standard uncertainty ($k = 1$) is shown in figures 6(a) and (b), respectively. Figure 6(a) shows that the radial dose function increases, reaches a maximum at about 1 mm–2 mm, and then decreases as the radial distance increases. Also, as can be seen in figure 6(b), at distances closer to the seed, the relative combined standard uncertainty in the measured radial dose function is about 1%–2%.

The 2D isodose distribution curves measured at 0.77 mm, 1.07 mm and 1.97 mm depths from the centre of the seed are displayed in figures 7(a), (b) and (c), respectively. For distances equal to 0.77 mm and 1.07 mm from the seed, a tail is observed, while at 1.97 mm, this tail is not noted. This could be associated with scattering produced by the catheter used as a stop to fix the position of the seed during the irradiation.

4. Discussion

The 3D dose distribution (DD) around a single intravascular brachytherapy $^{90}Sr/^{90}Y$ seed has been measured using gel dosimetry coupled with a special small format high-resolution laser CT scanner as the reading system. The results suggest that the relative DD can be measured very close to the seed with uncertainty as low as 1%–2%. Even though figure 6(b) shows uncertainty up to 10% at about 5 mm from the seed, better accuracy could be obtained if more measurements with longer irradiation times were performed (figure 4).

Figures 7(a), (b) and (c) indicate that the geometrical structure of the 2D DD for this seed changes as a function of depth. The DD is almost isotropic at approximately 2 mm depth,

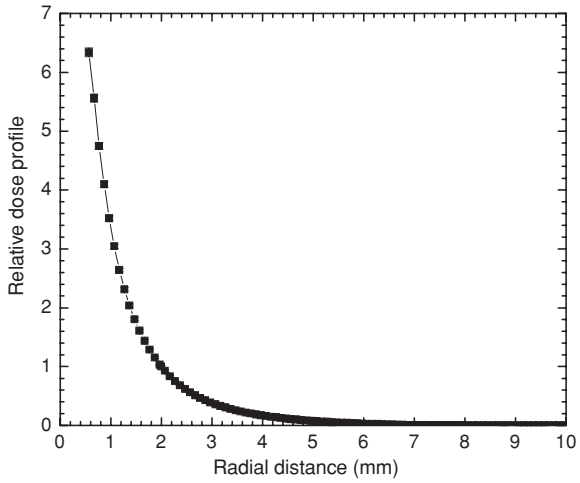

Figure 5. Relative dose profile for the $^{90}Sr/^{90}Y$ beta single source measured with the polymer gel.

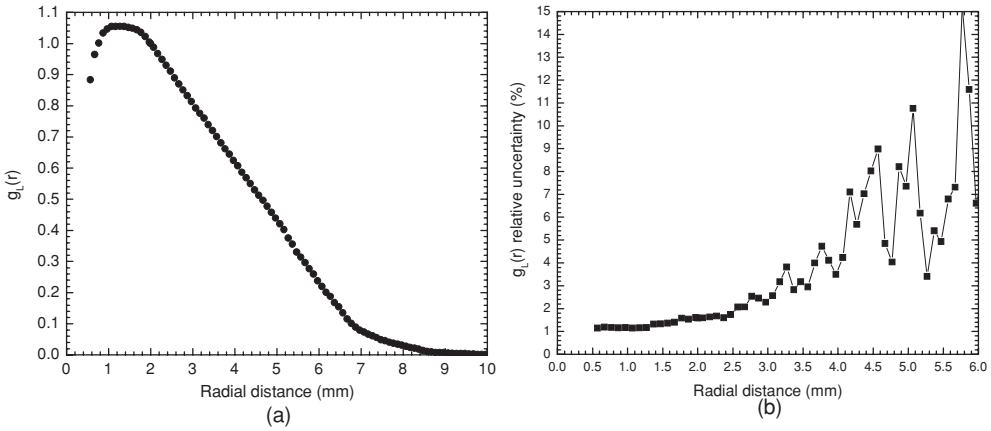

Figure 6. (a) Radial dose function measured for the $^{90}Sr/^{90}Y$ beta single source using the polymer gel. (b) Relative combined standard uncertainty of the measured radial dose function as a function of the radial distance.

which means that this seed can only be considered as a point source for distances larger than 2 mm from the seed. At about 0.77 mm depth, the DD has the source shape, i.e. it has a rectangular form, while at around 1.07 mm depth it looks like an ellipse. These effects might influence the anisotropy function at close distances to the seed. In addition, independent of the depth and the geometrical form, the DD is almost symmetric.

Figure 8(a) shows the radial dose function, $g_L(r)$, measured in this work compared with published data. It can be observed that our result is in good agreement with other measurements reported previously using thermoluminescent dosemeters (TLDs) and/or Gafchromic film (Soares *et al* 1998, Holmes *et al* 2006). Independent of the laboratory where the measurements were performed, no significant difference was observed between the Gafchromic film measurement and the gel. Although the TLDs underestimate the dose at distances less

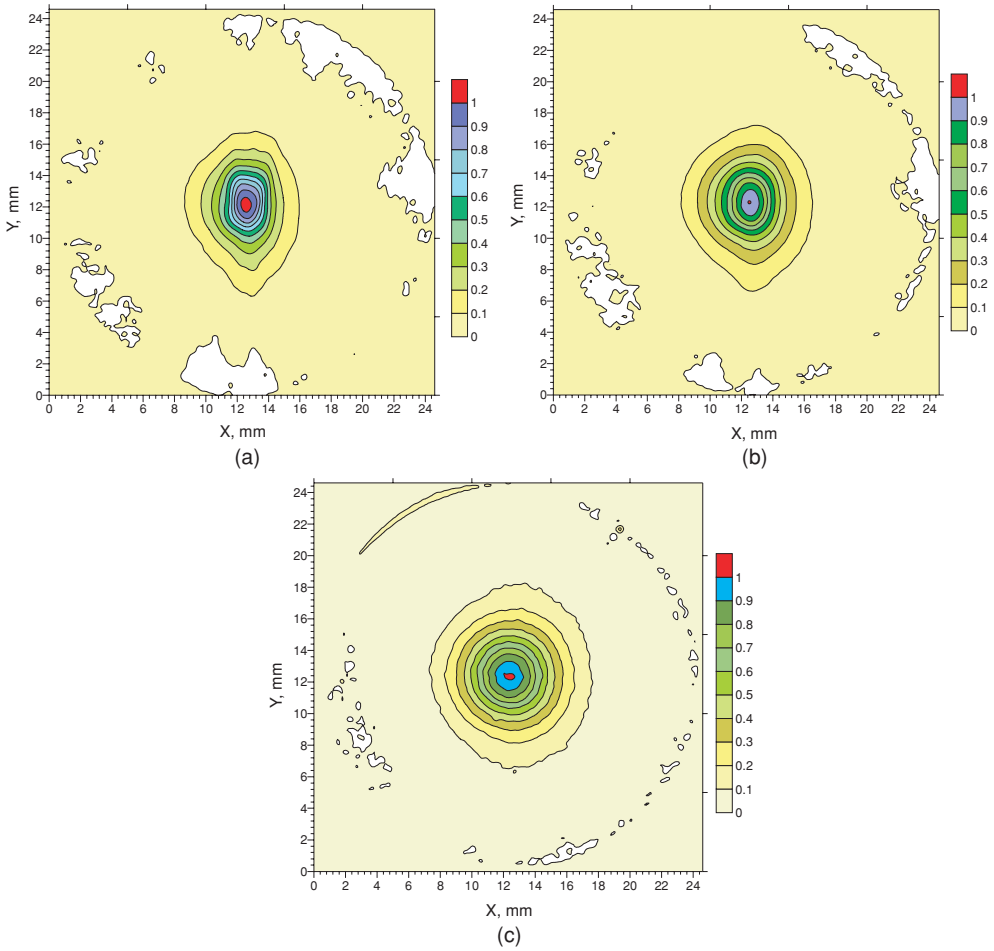

Figure 7. (a) 2D dose distribution measured at 0.77 mm depth from the centre of the seed. (b) Dose distribution measured at 1.07 mm depth. (c) 2D dose distribution measured at 1.97 mm depth.

than 1.5 mm from the seed, probably due to a volume averaging effect, all the experimental data follow the same behaviour. That is, starting at the seed position ($r = 0$), $g_L(r)$ increases as the distance increases up to approximately 1 mm, reaches a maximum and then decreases for larger distances. In contrast, the behaviour of $g_L(r)$ as a function of the radial distance obtained from published Monte Carlo simulations is quite different, as shown in figure 8(b). That is, calculated $g_L(r)$ functions do not predict a local maximum. Instead, starting with small values of the radial distance, the values of $g_L(r)$ decrease for increasing values of r. As seen in figures 8(a) and (b), the discrepancy between experimental and calculated values is found for radial distances smaller than 1.5 mm. Good agreement is obtained between the Monte Carlo simulations and the experimental data for distances ranging from 1.5 mm to 3.5 mm.

At distances less than 1.5 mm, differences of more than 20% can be observed between the experimental data and the Monte Carlo simulation. These discrepancies could be attributed to a possible underestimation of the energy lost by the electron spectrum due to the absorption

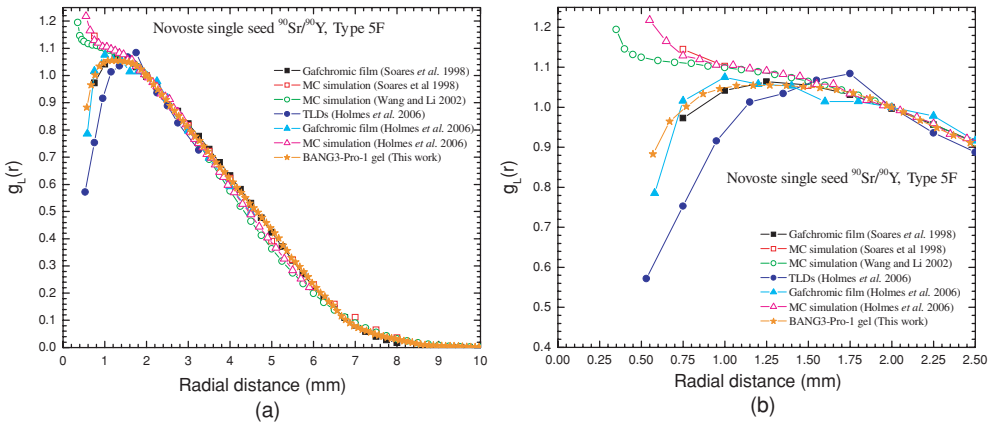

Figure 8. (a) Comparison of the radial dose function measured in this work with published data. (b) Short distance zoom of figure 8(a).

in the seed core and encapsulation during the Monte Carlo simulation, since the chemical composition of the core and its respective density for the 5F single seed are not well known. It has been reported that the ^{90}Sr/^{90}Y beta spectrum changes drastically with the mass thickness of the absorber material (Pruitt *et al* 1988). In the calculation made by Wang and Li, the core composition was assumed to be SiO_2 with a density of 3.0 g cm^{-3}, although they acknowledged that the density might be different (Wang and Li 2000, 2002). In their study, other calculations were performed with various core densities. They observed a decrease of more than 10% in $g_L(r)$ and a reduction of 16.3% in the dose per unit of contained activity at the reference position, if a density of 6 g cm^{-3} is considered (Wang and Li 2000). In parallel, Holmes and collaborators (Holmes *et al* 2006) reported that the composition of the seed used in their work was obtained through personal communication with Novoste. In this communication, the 5F source was assumed to have an inner ceramic matrix whose density can range from 2.6 g cm^{-3} to 4 g cm^{-3} with 48.4% Sr, 25.8% O and 25.8% Ti. Thus, a density of 2.6 g cm^{-3} was used and as can be observed in figure 8(b), the $g_L(r)$ obtained in that work had values close to the source that were even larger than those reported by Wang and Li. These facts confirm the importance of a precise knowledge of the core composition of the seed for Monte Carlo simulation; this, of course is not required for experimental measurements.

5. Conclusion

Experimental measurements using several different detection systems have been compared with Monte Carlo calculations. The experimental results are consistent in not agreeing with the Monte Carlo simulations at distances less than 1.5 mm. This indicates that Monte Carlo simulation cannot be considered as a good method to evaluate the dose distribution at distances of less than 1.5 mm around this seed and consequently, the radial dose function recommended by AAPM TG-149 (Chiu-Tsao *et al* 2007) for the 5F Novoste Beta-Cath ^{90}Sr/^{90}Y single source is not the best one available. Based on the measurements presented in this work and the above observations, we suggest that the radial dose function as recommended in the TG-149 protocol be revised.

The results presented in this work indicate that the polymer gel read with a laser CT scanner can be considered to be among the best methods currently available to measure the

dose distribution at close distances from an intravascular beta particle brachytherapy seed. These methods provide the high spatial resolution needed for beta dosimetry. Furthermore, polymer gel, besides being a tissue-equivalent dosemeter with a density equal to 1.03 g cm^{-3} (ICRU 2004, Massillon-JL *et al* 2009), has a very significant additional advantage: when used in conjunction with an optical CT scanner, it is able to measure the absorbed dose in three dimensions in one single measurement as opposed to other dosemeters, which require multiple planar measurements to obtain the 3D dose distribution. In addition, the gel provides a direct 3D physical visualization of the effect of the irradiation in the gel material.

References

Asenjo J, Fernández-Varea J and Sánchez Reyes A 2002 Characterization of a high dose rate ^{90}Sr-^{90}Y source for intravascular brachytherapy by using the Monte Carlo code PENELOPE *Phys. Med. Biol.* **47** 697–711

Brenner D J and Miller R C 2001 Long-term efficacy of intracoronary irradiation in inhibiting in-stent restenosis *Circulation* **103** 1330–2

Browne E 1997 *Nucl. Data Sheets* **82** 379

Chiu-Tsao S-T, Schaart D R, Soares C G and Nath R 2007 Dose calculation formalisms and consensus dosimetry parameters for intravascular brachytherapy dosimetry: recommendations of the AAPM therapy physics committee task group No. 149 *Med. Phys.* **34** 4126–57

Demir B, Ahmed A S, Babalik E, Demir M and Gürmen T 2008 Verification and uniformity control of doses for $^{90}Sr/^{90}Y$ intravascular brachytherapy sources using radiochromic film dosimetry *J. Med. Phys.* **33** 54–9

Duggan D M, Coffey II C W, Lobdell J L and Schell M C 1999 Radiochromic film dosimetry of a high dose rate beta source for intravascular brachytherapy *Med. Phys.* **26** 2461–4

Holmes S M, DeWerd L A and Micka J A 2006 Experimental determination of the radial dose function of $^{90}Sr/^{90}Y$ IVBT sources *Med. Phys.* **33** 3225–33

ICRU (International Commission on Radiation Units and Measurements) 2004 *Dosimetry of Beta Rays and Low-Energy Photons for Brachytherapy With Sealed Sources* (Oxford: Oxford University Press)

ImageJ Available online at http://rsbweb.nih.gov/ij/ August 2008

King S B III 1999 Restenosis following angioplasty: scope of the problem *Vascular Brachytherapy* 2nd edn ed R Waksman (Armonk, NY: Futura Publishing Company, Inc) pp 3–11

King S B III, Williams D O, Chougule P, Klein J L, Waksman R, Hilstead R, Macdonald J, Anderberg K and Crocker I R 1998 Endovascular β-radiation to reduce restenosis after coronary balloon angioplasty: result of the beta energy restenosis trial (BERT) *Circulation* **97** 2025–30

Li A X, Wang R, Yu C and Suntharalingam M 2000 Beta versus gamma for catheter-based intravascular brachytherapy: dosimetric perspectives in the presence of metallic stents and calcified plaques *Int. J. Radiat. Oncol. Biol. Phys.* **46** 1043–9

Maryanski M J, Gore J C, Kennan R P and Schulz R J 1993 NMR relaxation enhancement in gels polymerized and cross-linked by ionizing radiations: a new approach to 3-D dosimetry by MRI *Magn. Reson. Imaging* **11** 253–8

Maryanski M J, Schulz R J, Ibbott G S, Gatenby J C, Xie J, Horton D and Gore J C 1994 Magnetic resonance imaging of radiation dose distributions using a polymer-gel dosimeter *Phys. Med. Biol.* **39** 1437–55

Maryanski M J, Ibbott G S, Eastman P, Schulz R J and Gore J C 1996 Radiation therapy dosimetry using magnetic resonance imaging of polymer gels *Med. Phys.* **23** 699–705

Maryanski M J and Ranade 2001 Laser micro-beam CT scanning of dosimetry gels, medical imaging 2001: physics of medical imaging *Proc. SPIE 2001* ed L E Antonuk and M J Yaffe **4320** 764–74

Massillon-JL G, Minniti R, Mitch M, Maryanski M and Soares C 2008 New high-resolution method to measure the 3D dose distribution around brachytherapy seeds using BANG3-pro gel dosimetry *Med. Phys.* **35** 2920

Massillon-JL G, Minniti R, Soares C G, Maryanski M J and Robertson S 2009 Characteristics of the new polymer gel for high-ionization density dosimetry using a micro optical CT scanner *Med. Phys.* at press

Meerkin D, Tardif J-C, Crocker I R, Arsenault A, Joyal M, Lucier G, King S B III, Williams D O, Serruys P W and Bonan R 1999 Effect of intracoronary β-radiation therapy after coronary angioplasty: an intravascular ultrasound study *Circulation* **99** 1660–5

Ortolani P, Marzocchi A, Aquilina M, Gaiba W, Neri S, Marrozzini C, Palmerini T, Taglieri N and Branzi A 2005 ^{32}P Brachytherapy in the treatment of complex cypher in-stent restenosis *J. Interv. Cardiol.* **18** 205–11

Price M J, Giap H and Teirstein P S 2007 Intracoronary radiation therapy for multi-drug resistant in-stent restenosis: initial clinical experience *Cathet. Cardiovasc. Intervent.* **69** 132–4

Pruitt J S, Soares C G and Ehrlich M 1988 Calibration of beta-particle radiation instrumentation and sources *NBS Special Publication 250-51* (USA: NBS)

Rivard M J, Coursey B M, DeWerd L A, Hanson W F, Huq M S, Ibbott G S, Mitch M G, Nath R and Williamson J F 2004 Update of AAPM Task Group No. 43 Report: a revised AAPM protocol for brachytherapy dose calculations *Med. Phys.* **31** 633–74

Roa D E, Song H, Yue N, d'Errico F and Nath R 2004 Dosimetric characteristics of the Novoste Beta-Cath ^{90}Sr/Y source trains at submillimeter distances *Med. Phys.* **31** 1269–76

Soares C G, Halpern D G and Wang C-K 1998 Calibration and characterization of beta-particles sources for intravascular brachytherapy *Med. Phys.* **28** 1373–84

Wang R and Li X A 2000 A Monte Carlo calculation of dosimetric parameters of ^{90}Sr/^{90}Y and ^{192}Ir SS sources for intravascular brachytherapy *Med. Phys.* **27** 2528–35

Wang R and Li X A 2002 Dosimetric comparison of two ^{90}Sr/^{90}Y sources for intravascular brachytherapy: an EGSncr Monte Carlo calculation *Phys. Med. Biol.* **47** 4259–69

World Health Organization 2005 Chronic diseases and their common risk factors www.who.int/entity/chp/chronic_disease_report/media/Factsheet1.pdf available October 2008

Zeidan O A 2009 Personal communication